Journal of Himalayan Earth Sciences Volume 59, No. 1, 2026 pp. 51-69

Preliminary Paleomagnetic and Geodynamic Evidence for Vertical Axis Rotations in the Makran-Khojak Flysch Basin, Pakistan: Implications for India–Arabia–Eurasia Plate Interactions

Waseem Khan[1,2*], Ke Zhang[4,5], Ziying Li[1,2,3], Hao Liang[4,5], Mahnoor Mirwani[6], Jiangtao Nie[1,2,3], Jian Guo[1,2,3], and Shazia Fareed[7]

[1] Beijing Research Institute of Uranium Geology, Beijing 100029, China
[2] CNNC Key Laboratory of Uranium Resource Exploration and Evaluation Techniques, Beijing 100029, China
[3] National Key Laboratory of Uranium Resource Exploration-Mining and Nuclear Remote Sensing, Beijing, 100029, China
[4] Guangdong Provincial Key Laboratory of Geodynamics and Geohazards
[5] School of Earth Sciences and Engineering, Sun Yat-Sen University, Zhuhai, 519082, China
[6] Communication and Works, Physical and Housing Department, Government of Balochistan, Pakistan
[7] Department of Geology, University of Balochistan, Quetta, Pakistan
**Corresponding author: khanw@alumni.sysu.edu.cn , khan@briug.cn*

Submitted Date:28/11/2025 Acceptance Date: 12/01/2026 Publication Date: 31/03/2026

Abstract

The Makran-Khojak Flysch Basin (MKFB), situated in the northwest of the Indian Plate in Pakistan, exhibits a comprehensive sandstone sequence. This sequence has experienced significant tectonic bending and rotation due to orogeny during plate convergence. The MKFB is a compelling case study for examining the geological characteristics of an active convergent plate boundary marked by the oceanic lithosphere subduction. This is a preliminary investigation with specimen limitations, and the vertical axis rotations (VARs) obtained from preliminary paleomagnetic (PMag) data and geodynamic investigations offer a first-order constraint on the tectonic deformation within the MKFB. The findings show that the east-west trend rotated clockwise (CW) due to the subducting Arabian Plate underneath the Makran. The north-south trend rotated counter-clockwise (CCW) due to the main stress-strain driven by the Chaman fault in association with the northwest advance of the Indian Plate. The exception of CCW rotation of the GA section with < 1° acts as a transition zone, which has been influenced by the interactions between the Chagai-Raskoh Arc (CRA), Afghan Block, Arabian Plate, Indian Plate, and the Chaman Fault's strike-slip movement. Additionally, pre-depositional tectonic deformations occurred between the Arabian and Indian plates, with transpressional interactions bringing up an NNE-SSW convergence zone without any tectonic deformation in the Makran arc-trench gap until the late Eocene. While the post-depositional tectonic deformations of the MKFB occurred since the late Eocene, presenting the tectonic interactions between the Indian and Eurasian plates. Whereas the interactions between the Eurasian, Arabian, and Indian plates occurred throughout the Oligocene to late Miocene, which originated the Chaman Transform Fault. The results show that the MKFB formed as a minor symmetry typical of a Y-shaped junction during the Oligocene to Miocene.

***Keywords*:** *Makran-Khojak Flysch Basin; Chaman Fault; Arabian Plate; Indian Plate; Eurasian Plate.*

1. Introduction

The Makran-Khojak Flysch Basin (MKFB), at the NE of the Arabian Plate and NW of the Indian Plate in Pakistan, has developed a complete Oligocene-Miocene sandstone sequence that underwent strong tectonic bending and rotation with orogeny during plate convergence. The MKFB is a great case study for examining the architecture and geology of an active convergent plate margin where the oceanic lithosphere is being subducted. There have been limited studies conducted in the MKFB due to its inaccessibility and vast extension in Pakistan. These studies were limited to provenance-related investigations, e.g., Critelli et al. (1990), Kassi et al. (2015), Kakar et al. (2016), and Khan et al. (2023a; b). However, various seismological studies have been reported in offshore areas (e.g., Ellouz-Zimmermann et al., 2007; Mouchot et al., 2010). To date, no efforts have been carried out to examine potential VAR analysis and tectonic deformations by performing PMag analysis in the MKFB. Though few PMag studies were taken near Quetta and Loralai areas, they were limited to the Indian Plate (such as Klootwijk et al., 1981). Based on the previous research, it's hard to clearly understand the plate tectonic interaction, dynamics, and evolution in the area. Thus, the deformational behavior and tectonic history of the MKFB are subjects of ongoing debate. Therefore, understanding the evolution history of the MKFB is crucial for gaining comprehension of the tectonic phenomena associated with the interactions among the Eurasian, Arabian, and Indian plates and their inferences for regional tectonic history.

The characteristic features of the orogenic curvatures can be determined to examine the geometric phenomena and evolutionary processes by confining the magnitude and timing of tectonic rotations in bended orogeny, where thrust activities and VARs were reported (Sussman et al., 2004). Similarly, the preliminary PMag analysis is applied to MKFB to determine the propagation and magnitude of VARs. On the other hand, geodynamic numerical modeling can effectively calculate and simulate plate margin tectonic deformation and evolution. For the Indo-Eurasian plate collision and its boundary deformation process, various dynamic (or kinematic) models have been established. For example, a plane strain simulation of a rigid Indian plate indenter into the southern boundary of the Eurasian Plate (Tapponnier et al., 1982, 1986), a sandbox technique to examine the oblique convergence of the western edge of the Indian Plate (Haq and Davis, 1997), and a double indenter model to examine the tectonic deformation of the Tajik-Pamir region due to the collision of the Indian Plate (Reiter et al., 2011). Although the model of Haq and Davis (1997) is in the research area, it is limited to field-measured data and does not match the actual scenario of the MKFB tectonic evolution. In view of the existing problems, to better understand the deformation phenomenon and tectonic framework formation mechanism of the MKFB in plate convergence and to verify the results of PMag experiments, the paper establishes a 2-D geodynamic numerical model of the collision of the western boundary of the Indian Plate, which simulates the oblique collision and the resulting deformation and rotation phenomena.

By studying the preliminary PMag and geodynamic examinations, this research aims to provide insights into the PMag records and quantification of the first-order VARs and first integration with Abaqus modeling in the MKFB to discuss the large tectonic deformation. This paper further contributes to the understanding of the tectonic deformations originated from the Arabia-India oblique convergence, the Indian-Eurasian collision, and a shift from the India-Arabia oblique convergence to the Chaman strike-slip Fault by analyzing the Oligocene-Miocene-Pliocene sandstones and reconstructing the basin deformation process and restoring the tectonic evolution history by plate collision.

This study presents the first integrated paleomagnetic and geodynamic investigation

of vertical-axis rotations in the MKFB. Using 7 sampling sites across the basin and 2-D Abaqus modeling, we aim to: (1) quantify VAR magnitudes and directions, (2) relate rotation patterns to India–Arabia–Eurasia interactions, and (3) provide a preliminary tectonic model for the MKFB's deformation history.

2. Geological framework

The MKFB is an accretionary complex developed at the triple junction of the Arabian, Indian, and Eurasian plates (Khan et al., 2023b; 2026). Its structural and stratigraphic architecture records a prolonged history of oblique convergence, subduction, and strike-slip deformation (Khan et al., 2026). This section synthesizes the key geological elements of the MKFB, focusing on those most relevant to interpreting the paleomagnetic and geodynamic results presented in this study.

2.1 Tectonic setting and structural subdivision

The MKFB is divided into two dominant structural trends: the east-west-oriented Makran Flysch Basin (MFB) and the north-south-oriented Khojak Flysch Basin (KFB) (Fig. 1b; Khan et al., 2026). The basin is bounded to the east by the sinistral Ornach Nal Fault (ONF) and to the west by the dextral Menab fault in Iran (Fig. 1a). Three broad zones are recognized from north to south: (1) the Northern Outer Makran Zone, which includes the Cretaceous–Paleocene Chagai Raskoh arc (CRA) which is about 400 km off the coast of Makran; (2) the Central/Inner Makran Zone, dominated by Eocene–Miocene sedimentary rocks that form the core of the accretionary wedge and are mainly recycled from the orogeny and stratigraphic uplifted erosive sediments of the Indo-Eurasian plate collision (Khan et al., 2023b); and (3) the Coastal Makran Zone, comprising Pliocene–Pleistocene sediments that record the most recent frontal accretion (Khan et al., 2023b; 2026) (Fig. 1b).

The present-day structure results from the interplay of three major plate boundary processes: (1) northward subduction of the Arabian Plate beneath the Makran, (2) north-westward indentation of the Indian Plate, and (3) left-lateral strike-slip motion along the Chaman transform system (Khan et al., 2026). These processes have produced distinct deformation styles in the MFB (thrust-dominated) and KFB (transpressional), making the MKFB a natural laboratory for studying strain partitioning at a complex convergent margin.

2.2 Stratigraphy linked to deformation phases

The stratigraphic record of the MKFB can be grouped into three tectonic phases that correspond to changes in plate interaction dynamics (Fig. 1b)

2.2.1 Pre-depositional phase (Cretaceous–Paleocene)

Pre-collisional oceanic and arc-related rocks underlie the flysch sequence. Late Cretaceous shales, cherts, and volcaniclastics (CI Formation) are interpreted as remnants of the Neo-Tethyan Ocean floor. Paleocene conglomerates (TPI) containing quartzite, limestone, and volcanic clasts record initial uplift and erosion associated with the onset of India–Arabia convergence (Hunting Survey Corporation, 1960; Kassi et al., 2011, 2013, 2015; Khan et al., 2023a, b).

2.2.2 Syn depositional phase (Eocene–Oligocene to Early Miocene)

This interval contains the flysch units that were sampled for paleomagnetic analysis. The Late Eocene–Early Oligocene shales (TOMF) and (TEH) represent the oldest turbidite systems, deposited by the Paleo Indus River in a trench slope setting. During the Oligocene–Early Miocene, the basin received voluminous sand-rich turbidites of the (TOMP) and (TMS) formations, reflecting increased erosional input from the rising Himalayan–Karakoram orogen (Hunting Survey Corporation, 1960; Kassi et al., 2011, 2013, 2015; Khan et al., 2023a, b).

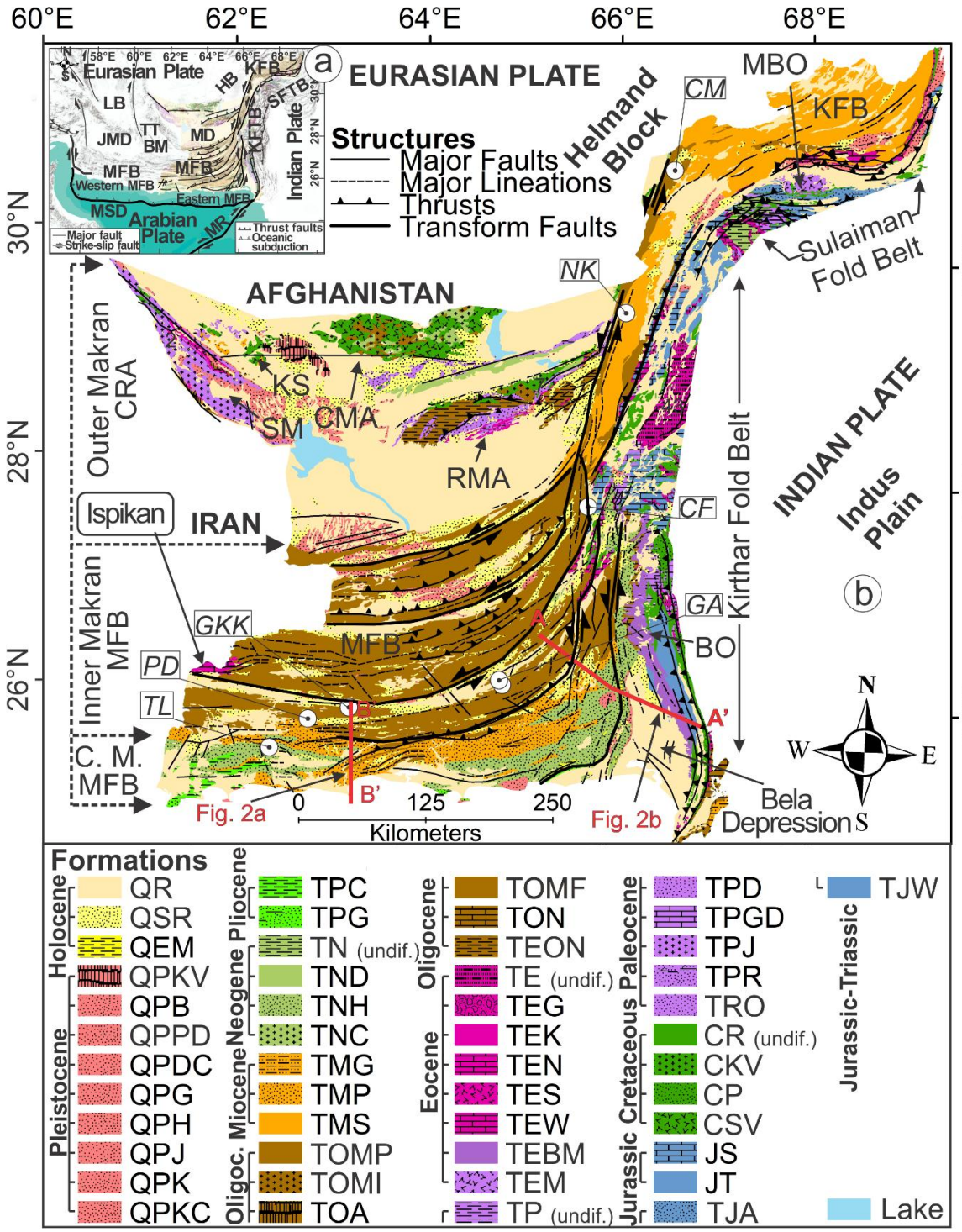

Fig. 1. Maps demonstrating (a) the inset of the regional structures (*LB: Lut Block, JMD: Jaz Murian Depression, HB: Helmand Block, MSD: Makran Subduction Zone, MR: Murray Ridge, MD: Mashkhel Depression, TT: Taftan, BM: Bazman*), and (b) the stratigraphy and structure of the basin and adjacent areas in southwest Pakistan with sampling spots (*CRMA: Chagai-Raskoh Magmatic Arc (CA+RA+KSA+SMA), CA: Chagai Arc, RA: Raskoh Arc, KS: Koh-e-Sultan Arc, SA: Saindak Arc, MFB: Makran Flysch Basin, KFB: Khojak Flysch Basin, BO: Bela Ophiolites, MO: Muslimbagh Ophiolite, QR: Recent-deposits, QSR: Sub-recent deposits, QEM: Pleistocene mud deposits , QPKV: Pleistocene Koh-i-Sultan volcanic rocks, QPB: Bostan Formation, QPPD Pleistocene Piedmont deposits derived from adjacent highlands, QPDC: Pleistocene Dada Conglomerate, QPG: Pleistocene Gwalishtap Formation, QPH: Pleistocene Haro Conglomerate, QPJ: Pleistocene Jiwani Formation, QPK: Pleistocene*

Kamerod Formation, QPKC: Pleistocene Kech Conglomerate, TPC: Pliocene Chatti Formation, TPG: Pliocene Gwadar Formation, TN (Undif.): Neogene undifferentiated rocks, TND: Neogene Dalbandin Formation, TNH: Neogene Hinglaj Formation, TNC: Neogene Chaudwan Formation (in Kirthar belt) and Chagai granite (in Chagai), TMG: Miocene Gaj Formation, TMP: Miocene Parkini Formation, TMS: Miocene Shaigalu Formation, TOMP: Oligocene-Miocene Panjgur Formation, TOMI: Oligocene-Miocene intrusive, TOA: Oligocene Amalaf Formation, TOMF: Oligocene-Miocene Murgha Faqirzai Formation, TON: Oligocene Nari Formation and Nal limestone, TEON: Eocene-Oligocene Nauroz Formation, TE (Undif.): Eocene undifferentiated rocks, TEG: Eocene Ghazij Formation, TEK: Eocene Kirthar Formation (in Kirthar) and Kharan Formation (in Raskoh), TEN: Eocene Nisai Formation, TES: Eocene Saindak Formation, TEW: Eocene Wakai Limestone, TEMB: Eocene Muslimbag and Bela Ophiolites and Mélanges, TEM: Eocene Ophiolitic mélange, TP (Undif.): Paleocene undifferentiated rocks, TPD: Paleocene Dungan Formation, TPGD: Paleocene Gidar Dhor Formation, TPJ: Paleocene Juzzak Formation, TPR: Paleocene Bara/Khadro/Lakhra Formations, TRO: Paleocene Raskoh Ophiolite, CR (Undif.): Cretaceous undifferentiated rocks, CKV: Cretaceous Kuchakki volcanic rocks, CP: Cretaceous Pab Formation, CSV: Cretaceous Sanjirani volcanic rocks, JS: Jurassic Shrinab Formation, JT: Jurassic Takatu Formation, TJA: Triassic-Jurassic Alozai Group and equivalent, TJW: Triassic-Jurassic Windar Formation).

These units are characterized by well-bedded, often coarse-grained sandstones interlayered with mudstones, providing suitable lithologies for paleomagnetic investigation.

2.2.3 Post depositional phase (Miocene–Quaternary)

From the Middle Miocene onward, the MKFB underwent intense shortening and uplift. The mudstone-dominated (TMP) and (TMG) display progressive deformation, including tight folding and thrust repetition. Pliocene–Pleistocene shallow marine and coastal deposits (TPG, TPC, QR) cap the sequence and are themselves folded, indicating that contractional deformation has continued into the recent past (Ellouz-Zimmermann et al., 2007; Kassi et al., 2011, 2013, 2015; Khan et al., 2023a, b).

The paleomagnetic samples analyzed in this study were collected from the Oligocene–Miocene sandstones (TOMP, TMS, TMP) that recorded the primary phase of India–Eurasia convergence and the subsequent rotational deformation.

2.3 Regional tectonic architecture

Two representative cross sections illustrate the contrasting structural styles across the MKFB (Fig. 2).

2.3.1 N–S profile

This section across the Coastal Makran Range shows a south-vergent imbricate thrust system propagating over a basal detachment within Cretaceous–Paleocene abyssal strata (Fig. 2a). Late Miocene turbidites are intensely folded, with local back thrusts and overturned limbs, reflecting ongoing frontal accretion (Ellouz-Zimmermann et al., 2007).

2.3.2 E–W profile

This section reveals along-strike variations in deformation (Fig. 2b). From west to east, the detachment steps up to younger stratigraphic levels, and the structural style transitions from thrust-dominated shortening to transpressional deformation near the ONF. En échelon folds and mud volcanoes near the Bela Depression indicate strike-slip influence and fluid overpressure (Delisle et al., 2002; Ellouz-Zimmermann et al., 2007).

These profiles provide the structural context for interpreting the paleomagnetic rotations: the north–south section reflects accretion-related shortening, while the east–west section illustrates the strain gradient imposed by the oblique convergence of the Indian Plate and the left lateral Chaman system.

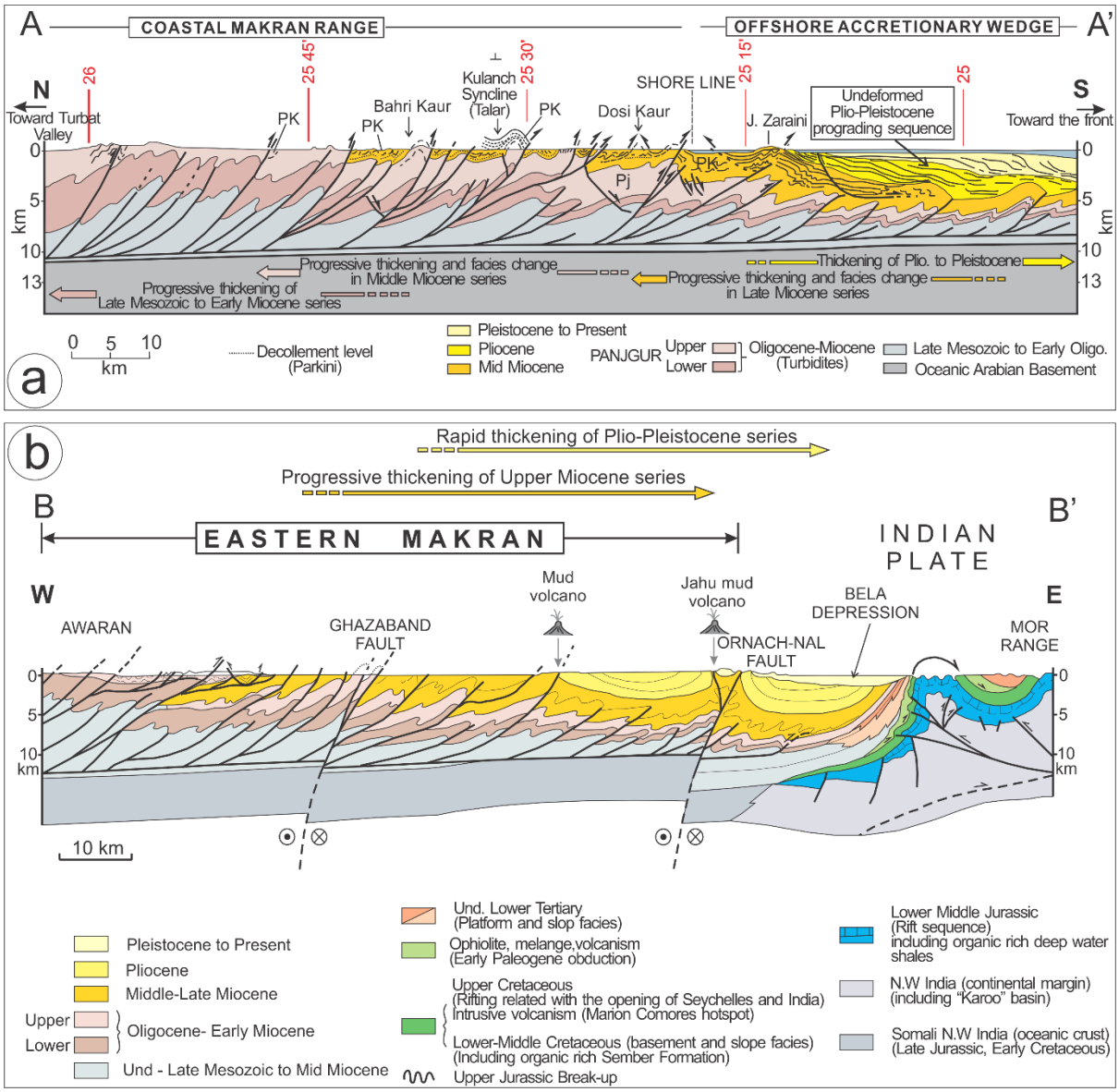

Fig. 2. Regional tectonic profiles of the Makran. (a) North-south regional tectonic profile (modified after Ellouz-Zimmermann et al., 2007). The stratigraphic age of the detachment zone is not clear, but it is likely to occur in the Paleocene or older deep-sea series. Note: (i) the accretive wedge is strongly deformed and thrust southward over the Late Miocene series; (ii) the local detachment makes the basement of the Parkini Formation strongly incongruous; and (iii) normal faults occur in the south, and the faults gradually become new to the south. (b) East-west tectonic profile (modified after Ellouz-Zimmermann et al., 2007). Where the Parkini Formation is mainly exposed in the anticline core and is sometimes brought to the surface from deep by mud-volcanic belts, showing strong disharmony. It is noteworthy that there are also large sedimentary centers along the Bela depression, which have accumulated a large number of sandstone units since the Pliocene, and the late accumulation wedge is offset by transform faults.

3. Materials and methods

A total of seven locations were selected for sampling in the MKFB. Samples were collected from Talar in the southwest of Kech district (TL), Pidark in the south of Turbat city (PD), Garakken in Sami-Kech (GKK), Gushanag in Awaran district (GA), Chaman Fault in Basima (CF), Noshki village (NK), and Khojak Pass in Chaman (CM) (Fig. 1b). After recording the structural

orientations in the field, the block samples were collected and transported to the laboratory. The samples were drilled to obtain cylindrical specimens with a diameter of 2 cm and a length of 2.2 cm. A total of 105 samples from 7 sections were selected for paleomagnetic (PMag) analysis after initial reliability screening.

The experiments were jointly completed at the School of Earth Sciences and Engineering, Sun Yat-sen University, and the Beijing Research Institute of Uranium Geology, China. Thermal demagnetization was performed using a Schonstedt oven, with a residual magnetic field of <10 nT inside the cooling chamber. Each sample underwent a 14–18-step thermal demagnetization test. The maximum demagnetization temperature of most of the samples was 580 °C, and for hematite-containing samples, it was up to 680 °C. Magnetic remanence was measured with a 2G 3-axis cryogenic magnetometer. All demagnetization and remanence measurements were performed in a magnetically shielded room with residual fields of less than 300 nT. The post-PMag laboratory examinations were calculated by paleomagnetism.org (Koymans et al., 2016) web portal. After tilt correction and conversion from reverse to normal polarity, the Fisher-site mean statistics were run by the PaleoMac (Cogné, 2003). Reliability criteria were evaluated using the procedures of Butler (1992). Due to intense thrusting and lack of distinguishable fold limbs in the region, a fold test or pre-tilt correction was not feasible. This limitation is acknowledged, and the results are interpreted as post-folding magnetizations. The geodynamic modeling was performed in the Abaqus/CAE 2022 environment.

4. Results

4.1 Demagnetization and Fisher site-mean directions

Most samples yielded two to three magnetization components. A low-temperature component was removed between 100–300 °C, whereas the high-temperature component above ~300 °C decayed toward the origin. The unblocking temperatures (425–530°C) suggest magnetite as the dominant carrier. However, given the region's volcanic and hydrothermal activity, partial re-magnetization cannot be ruled out. The consistency of high-temperature components across sites supports a primary or early diagenetic origin (Fig. 3).

For each specimen, three to six consecutive demagnetization steps were used to calculate the directions of the high-temperature component. To ensure reliable rotation estimates, only characteristic remanent magnetization (ChRM) directions with maximum angular deviation (MAD) $\leq 15^{o}$ were accepted. The site-mean directions, before and after tilt corrections, are presented in Fig. 4 and Table 1.

4.2 VARs analysis

The TL section exhibits a CW rotation angle of 18.78° ± 2.2°, the PD section shows a CW rotation angle of 24.35° ± 3.0°, and the GKK section records a CW rotation angle of 63.90° ± 3.0°. The GA section indicates a CCW rotation angle of -0.69° ± 3.0°, whereas the CF, NK, and CM sections show progressively increasing CCW rotation angles of –14.46°, –32.21°, and –67.45°, respectively (Fig. 5 and Table 1).

5. Discussion

5.1 VARs analysis

This preliminary analysis is limited by specimen availability; however, the VARs derived from preliminary PMag data and geodynamic studies provide a first-order constraint on the tectonic deformation within the MKFB. Based on the preliminary PMag results, combined with plate-interaction patterns, the study area can be divided into two structural trends: (1) east-west and (2) north-south trends. The east-west trend includes three sections, TL, PD, and GKK, reflecting the interaction between the Arabian plate and MKFB. The north-south trend includes three sections, CF, NK, and CM, reflecting the interaction between the Indian plate and MKFB and the strike-slip

motion of the Chaman Fault. The GA section's minimal rotation (<1°) coincides with a zone of fault density changes and mixed fold vergence observed in field studies (Khan et al., 2023b; 2025; this study), supporting its role as a kinematic transition between the E-W and N-S rotational domains (Figs. 1 and 5).

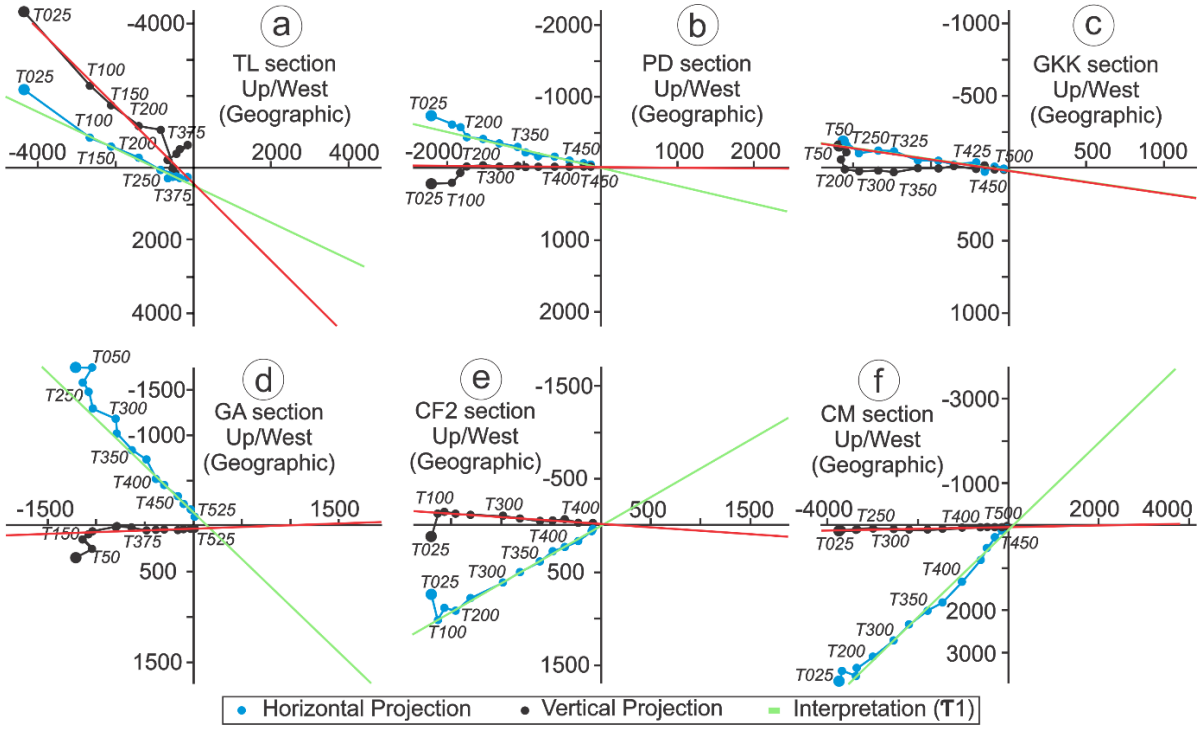

Fig. 3. Selected Zijderveld diagrams from six sections, plotted in geographic coordinates. (a) Talar section, (b) Pidark section, (c) Garakken section, (d) Gushanag Awaran section, (e) Chaman Fault in Basima section, and (f) Khojak Pass in Chaman section.

Table 1: The calculated vertical-axis rotation analysis of the Makran-Khojak Flysch Basin

		Site Location		Observed Direction			Expected Direction			Pl Reference			Rotation	
ID	N	Lat	Lon	Dec	Inc	α 95	Dec	Inc	α95	Dec	Inc	α95	R	ΔR
TL	3/3	25.60	62.70	24.08	5.94	13.74	5.3	41.9	2.1	168.1	85.0	2.0	18.8	2.2
PD	7/9	25.87	63.07	31.55	58.89	7.70	7.2	42.3	2.8	164.2	83.3	2.7	24.4	3.0
GKK	2/8	25.99	63.47	71.11	39.65	12.83	7.2	42.4	2.8	164.2	83.3	2.7	63.9	3.0
GA	4/7	26.28	64.93	6.61	32.26	14.55	7.3	43.0	2.8	164.2	83.3	2.7	-0.7	3.0
CF	4/9	27.00	65.00	-7.06	32.10	14.18	7.4	45.1	2.7	164.2	83.3	2.7	-14.4	3.0
NK	2/3	29.00	66.00	-25.71	52.34	11.38	7.5	47.3	2.6	164.2	83.3	2.7	-33.2	3.1
CM	3/9	30.00	66.00	-59.75	41.46	12.39	7.7	48.8	2.5	164.2	83.3	2.7	-67.4	3.1

N represents the number of specimens selected after final interpretation, Lat represents latitude, Lon represents longitude, Dec represents declination, Inc represents inclination (from Fisher, 1953), α95 represents the uncertainty (from Fisher, 1953), Pl represents paleopole latitude, R represents rotation angle, and ΔR represents uncertainty of rotation angle. Note that no normal polarity was observed; the observed directions are represented after correction of reverse polarity. Note that Late Miocene mudstone samples were collected from the TL section, and Late Oligocene to Early Miocene sandstone samples were collected from the rest of the sections.

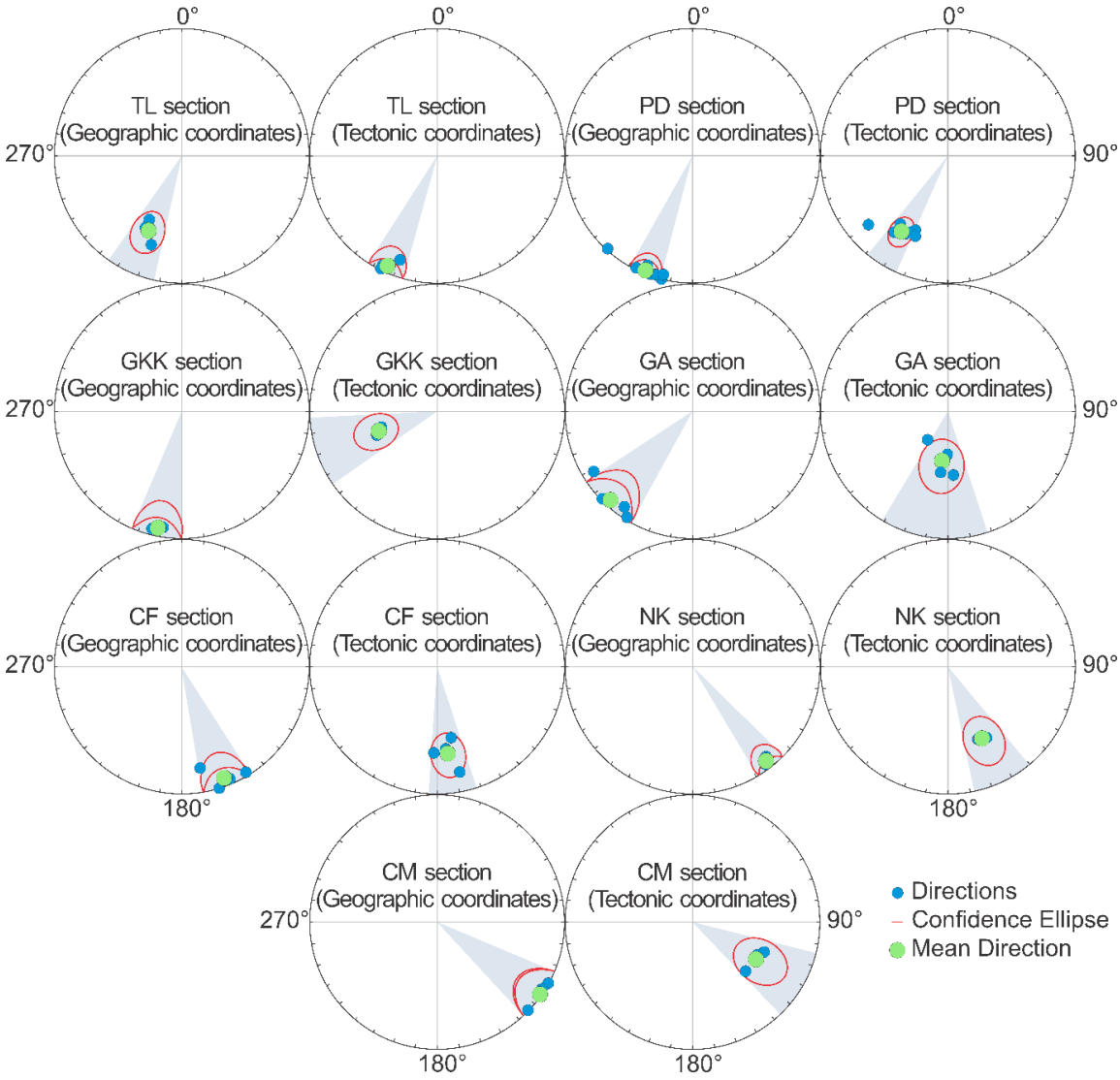

Fig. 4. The site-mean directions of the seven sections are shown, where, geographic coordinates represent in-situ directions and tectonic coordinates represent the tilt-corrected directions. TL: Talar section, PD: Pidark section, GKK: Garakken section, GA: Gushanag Awaran section, CF: Chaman Fault in Basima section, NK: Noshki section, and CM: Khojak Pass in Chaman section.

5.1.1 East-west trend

The tectonic rotation recorded along the east–west MFB remains debated. Earlier studies attribute variations to factors such as subduction zone geometry, Arabian-Eurasian plate convergence rate, and the stress-strain dispersal within the MFB (e.g., Besse and Courtillot, 1988). This study represents CW rotations of the east-west trend in MFTB with a maximum calculated total compass angle of 63.91 degrees (Fig. 5). Because the northward advance of the Indian Plate exerts relatively little compressional influence on the southwestern Makran, the CW rotation was mainly associated with the Arabian Plate's subduction towards the MFB and internal strike-slip mechanisms within the fold-thrust system. The CW rotation of the E-W trend likely results from strain partitioning due to oblique subduction of the Arabian Plate beneath the Makran, coupled with buttressing against the Chaman transform system (Ellouz-Zimmermann et al., 2007).

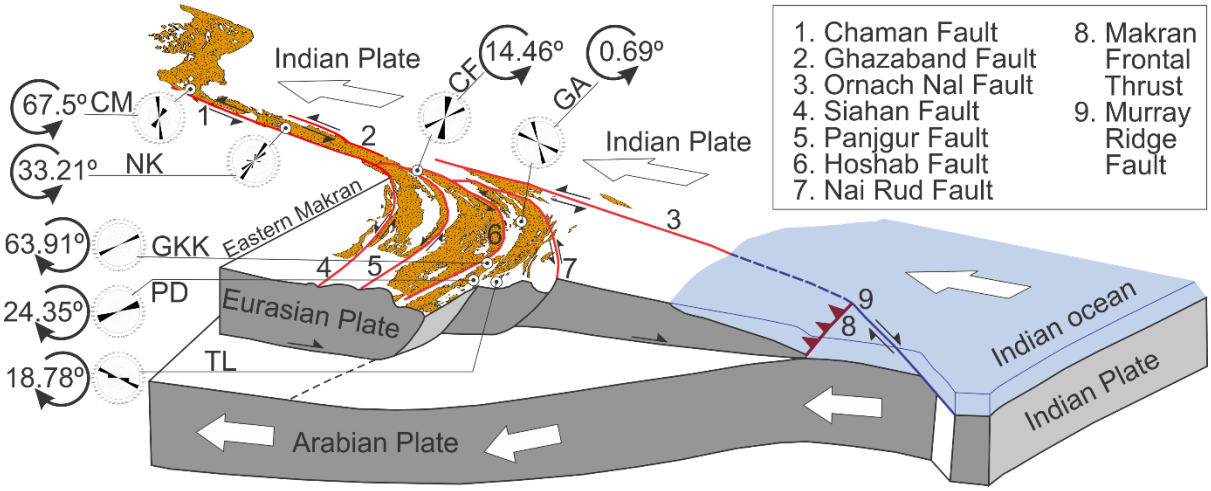

Fig. 5. Tectonic block model displaying the amount of rotated angle of different sections of the Makran-Khojak Flysch Basin and the interactions of the plates (modified after Khan et al., 2026). *TL: Talar section, PD: Pidark section, GKK: Garrakken section, GA: Gushanag Awaran section, CF: Chaman Fault section in Basima, NK: Noshki section, CM: Khojak Pass in Chaman.*

5.1.2 North-South trend

Since the Miocene, the Indian and the Eurasian plates have converged obliquely, producing transpressional deformation on both sides of the Chaman strike-slip Fault along the northwest edge of the Indian plate (Gaina et al., 2015). The CCW tectonic rotation shown by the CF section is clearly associated with northward underthrusting of the Indian Plate and strain partitioning along the western plate boundary, including the Chaman Fault (Fig. 5). Although Klootwijk et al. (1981) reported no significant tectonic rotations from paleomagnetic studies in the northern Kirthar Mountains east of the CF section, this area lies outside the Indian Plate and has limited tectonic influence on the study region. Consequently, rotation within the CF section is more likely related to northward Indian Plate advance and shortening associated with the development of the Chaman strike-slip fault (Fig. 5).

NK samples were collected from the Chaman Fault at the juncture of the CRA, Afghan Block, and Indian Plate. Gaina et al. (2015) noted that the Chaman Fault dominates the strong oblique strain distribution between the Afghan Block and the Indian plate. This further confirms the results of the CCW rotations of the NK section, i.e., the strike-slip motion along the Chaman Fault regulates the crustal shortening produced by Indian Plate subduction (Fig. 5). This section is influenced by both the counterclockwise rotation of the Helmand block and the clockwise rotation of the CRA. These opposing tectonic stresses concentrate deformation in the NK area and limit the rotation amplitude of the NK section.

During the Pliocene to Pleistocene, the Loralai-Sulaiman Mountains experienced a CW rotation of ~50° relative to the Indian Plate (Klootwijk et al., 1981), which is coordinated with the strike-slip movement of the Chaman Fault, the CCW rotation of the Afghan Block, and the CCW rotations of the Miocene-Pleistocene CM section (Fig. 5). It is inferred that the CM section located in the north-south tectonic belt therefore records a significant CCW rotation of 67.45° (Fig. 5).

5.2 Deformation and displacement of the western Indian margin

The simulation results show that the MKFB has two continuous and gradual stages, corresponding to two geological time scales, namely the late Eocene–early Miocene and the Miocene–present. The Late Eocene-Early Miocene displacements begin in the initial period (i.e., 100 to 600 steps in

units) (Fig. 6a), while the Miocene-present displacements occur in periods 700 to 1000 steps in units (Fig. 6b). During the Late Eocene–Early Miocene, India converged obliquely relative to the Eurasian Plate, which produced only low displacement rates, whereas displacement markedly increased during the Meso-Miocene–present stage. The continuous oblique convergence of the Indian Plate progressively divided the originally continuous MKFB into the MFB and KFB, producing a left-lateral displacement junction along the central part of the Chaman transform fault system (Fig. 6b).

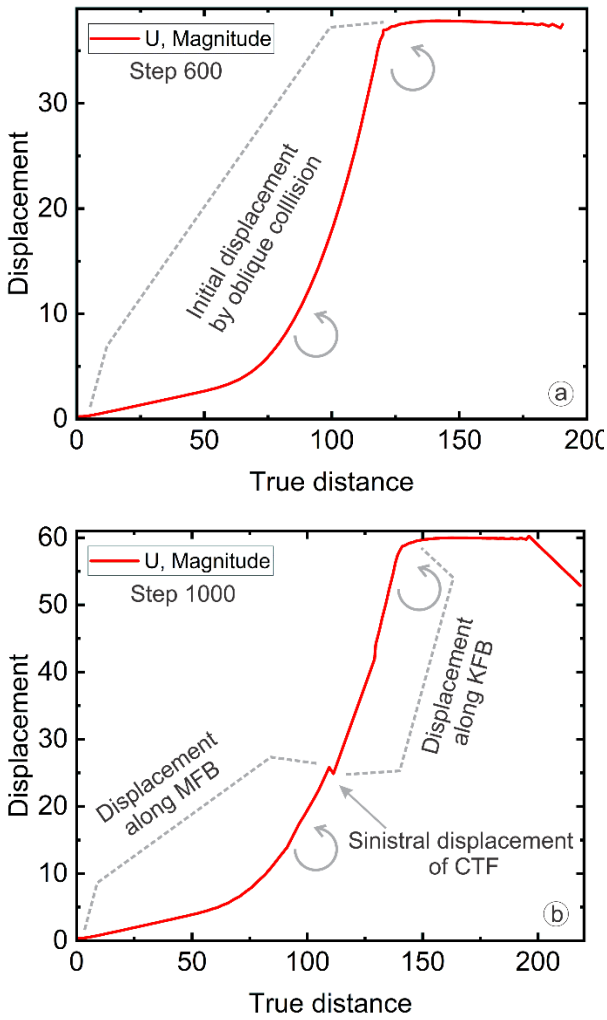

Fig. 6. The diagrams showing (a) the biplot of the displacement vs. true distance along path at step time 600 and (b) the biplot of the displacement vs. true distance along path at step time 1000 (final stage: this study). MFB: Makran Flysch Basin, KFB: Khojak Flysch Basin, CTF: Chaman Transform Fault.

Due to the oblique convergence of India relative to the Eurasian Plate, PMag VARs indicate a CCW rotation of the MKFB between the Eurasian and Indian plates (Fig. 5), and geodynamic models also show a gradual CCW rotation of the MKFB (Figs. 7 and S2). The PMag-VAR results demonstrate that the CCW rotation gradually increased from south to north, among which the highest rotation (-67.4° ± 3.1°) was recorded at the CM section. The geodynamic simulations show the highest displacement concentrated in the northern curvature of the system, confirming that the CM section exhibits the strongest CCW rotation (Fig. 7).

5.3 Typical Y-shaped tectonic genesis (splay faulting)

Since the Eocene, the extent to which the Eurasian lithosphere has accommodated deformation through shortening, thickening, and strike-slip motion during collision with the Indian Plate remains debated. Tapponnier et al. (1986) proposed a rigid extrusion model to explain continental deformation and collision-related large-scale strike-slip motion, demonstrating that strike-slip displacement can offset suture-zone markers (e.g., mélanges, ophiolites, and flysch) and generate Y-shaped junctions between true sutures and strike-slip–related pseudo-sutures. Geodynamic simulations of this paper do show the possibility of this mechanism, i.e., the Indian Plate's oblique collision relative to the Helmand Block led to the development of Y-shaped suture zones (Fig. 8a), which is consistent with the PMag results, where left-lateral strike-slip or CCW rotation occurs in the north-south segment of the MKFB (Fig. 5). Later, it possibly transferred into splay faulting (Fig. 8a).

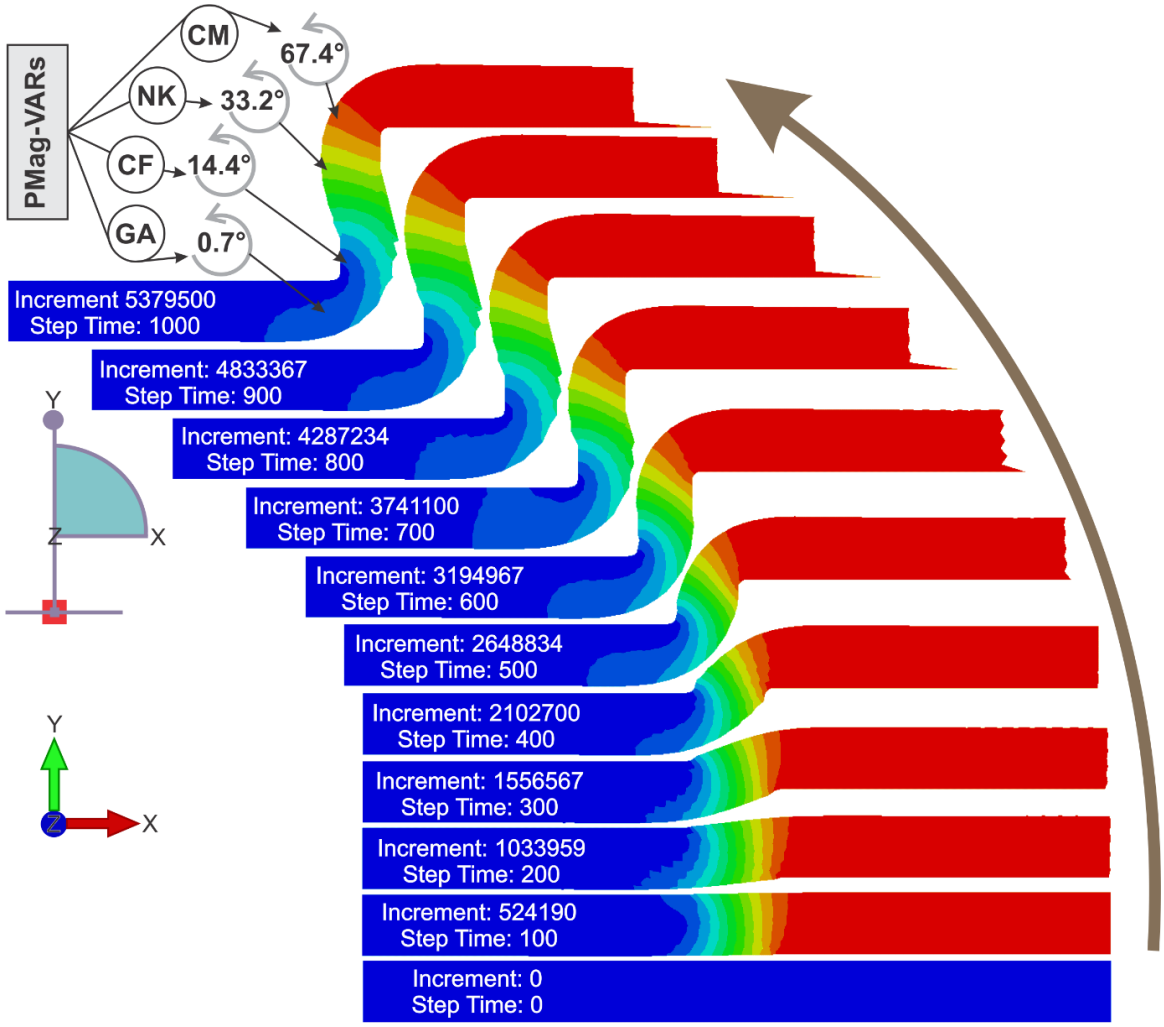

Fig. 7. The model of the MKFB geodynamic displacement caused by the oblique collision of the Indian and Eurasian plates.

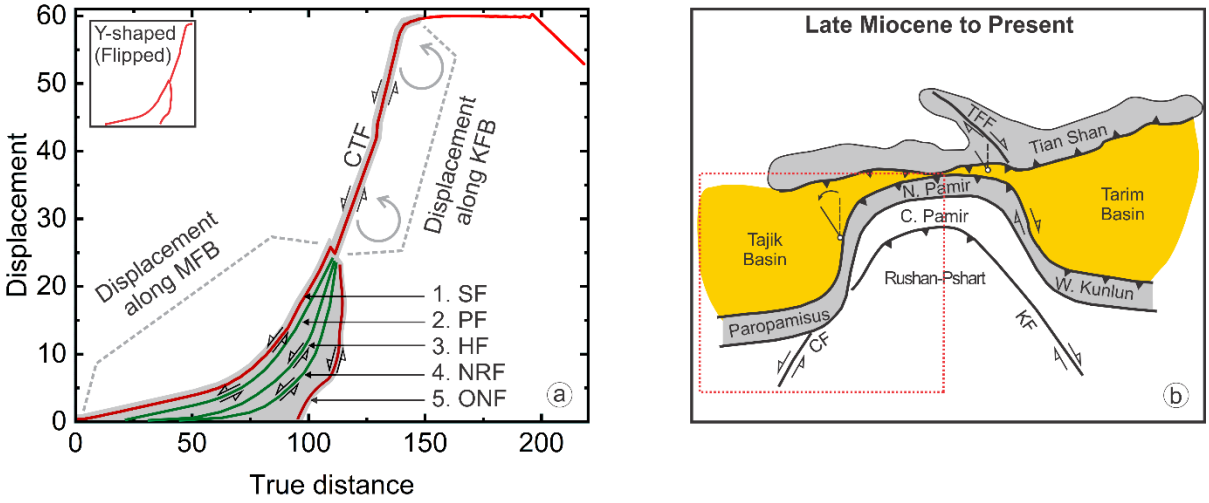

Fig. 8. The diagrams showing (a) the proposed displacement and the dispersion of the left lateral strike-slip faults and (b) the evolution model of the Pamir (after Zhang and Sun, 2020). MFB: Makran Flysch Basin, KFB: Khojak Flysch Basin, CTF: Chaman Transform Fault, CF: Chaman Fault, SF: Siahan Fault, PF: Panjgur Fault, ONF: Onrnach Nal Fault, NRF: Nai Rud Fault, HF: Hoshab Fault, KF: Kunlun Fault, TFF: Talas Ferghana Fault.

5.4 Pre-depositional tectonic deformations of the MKFB

Based on plate tectonic reconstructions in the Indian Ocean, there have been several extensions and compression events between the northwest/west Indian and the Arabian plates since the Jurassic, with the longest lasting occurring in Cretaceous-Eocene, forming an NNE-SSW subduction zone between the Indian and Arabian plates (Gaina et al., 2015). The formation of the Muslimbagh ophiolite (MBO) during the Late Cretaceous indicates that the Indian Plate started subducting towards the Arabian plate at least 80 Ma ago. It is worth noting that the geochemical characteristics of the MBO subduction zone given by Khan et al. (2007) indicate that the whole ophiolitic body is similar in age.

In addition, with the opening of the Red Sea and the Carlsberg Ridge, the Arabian Plate collided with the Iranian block and then with the CRA, an event that lasted from the Cretaceous to the Paleocene, resulting in strong tectonic deformation of the southern margin of the Eurasian Plate.

The Arabian and Indian plates converged strongly, obliquely, ~63 Ma to 50 Ma ago. According to the Bela ophiolite and the MBO metamorphic sole dating (65Ma, Mahmood et al., 1995; Gnos et al., 1998) and the continued expansion of the pre-arc basin of parallel trenches (Dewey and Casey, 2011). It can be deduced that the Indian Plate has subducted with respect to the Arabian Plate at this time, while the Bela ophiolite and MBO were moved to the continental margin of the Indian Plate. From 65 Ma to 55 Ma, the Masirah ophiolitic body was strongly uplifted over the Arabian Plate margin and thrusted (Immenhauser et al., 2000), indicating that two thrust/subduction systems have formed at the Indian and Arabian plate boundaries.

In the Early Eocene, the Indian Plate's northward advancement decreased sharply, and the relative velocity of motion between the Arabian and Indian plates decreased (Molnar and Stock, 2009; Copley et al., 2010; van Hinsbergen et al., 2011). Suo et al. (2022) argued that the continent-continent collision at 41–38 Ma created the Himalayan orogeny, slowing the Indian Plate's northward advancement. The Arabian Plate, on the other hand, continued its rapid northeasterly movement and eventually collided obliquely with the Indian Plate in the east and the Afghan Block in the north (Fig. 9a).

5.5 Post-depositional tectonic deformations of the MKFB

The results of this study are similar to the geometric morphology and physical characteristics of the Tajik basin. The tectonic features of the MKFB and the Tajik-Pamir basin show an arc shape (Fig. 8b), in which the Tajik-Pamir basin bends and strikes in east-west mirror symmetry (Cowgill et al., 2003; Robinson et al., 2004; Cowgill, 2010; Burtman, 2013; Bosboom et al., 2014; Bande et al., 2017; supported by Zhang and Sun, 2020), while the MKFB (Fig. 8b) corresponds to the western Tajik-Pamir basin. The tectonic evolution of the MKFB is similar to that of the Tajik-Pamir basins and is categorized into three stages of Late Eocene-Oligocene, Late Oligocene-Miocene, and Miocene-present.

5.5.1 Late Eocene-Oligocene

The MKFB was an arc-trench basin, and there was no sedimentation earlier than the Late Eocene (Khan et al., 2023b). As the Indian plate moved northward, sediments were transported by the Paleo-Indus River at the western edge of the Indian Plate to the MKFB arc-trench basin, and the TOMF (Fig. 9a) was deposited in the KFB basin, which underwent longitudinal displacement to form the Hoshab shale. Due to the Indian Plate's oblique collision relative to the Helmand Block, the MKFB began to move northwest and rotated CCW.

5.5.2 Late Oligocene-Miocene

The sediments derived from the Kohistan Ladakh arc (including Murgha Faqirzai, Hoshab, Panjgur, Shaigalu, and others) were deposited in the MKFB via the Paleo-Indus River. The TOMP was deposited

parallel to the Hoshab Shale (TEH) in the Miocene. The collision of the northwest edge of the Indian Plate with the Helmand Block caused the ophiolites to be moved to the northwestern edge of the Indian Plate. Studies by Haq and Davis (1997) and Jadoon and Frisch (1997), further indicated that from the Late Oligocene to Miocene, the crust between the Afghan Block and the Indian Plate was strongly shortened until MKFB finally formed, forming a suture zone between the Indian Plate and the Afghan Block (Tapponnier et al., 1981; Treloar and Izatt, 1993), and moved the BO and MBO to the western rim of the Indian plate and observed strong deformation and shortening. In addition, the converging strike-slip between the Indo-Arabian plates was converted into a left-lateral strike-slip motion of the Chaman transform fault (towards the NNE-SSW, formed during the Late Cretaceous to Early Eocene extrusion event) and formed the MKFB (Figs. 9a and 9b).

Similarly, in the MKFB, the Indian plate continued to rotate CCW (Treloar and Izatt, 1993) and finally started the left-lateral strike-slip of the Chaman transform fault at about 25 Ma (Ul-Hadi, 2012).

5.5.3 Miocene-present

Subduction reactivated at the southern Makran as the continental lithospheric plate subducted into the Eurasian plate and accelerated in the late Miocene (Figs. 9b and 9c) (Lawrence et al., 1981). The MKFB deposition ended with the continuous oblique convergence of the Arabian Plate, resulting in the strongest tectonic movement and strong fold-thrust (Fig. 9d), where a large number of new sediments from the late Miocene to the Holocene were deposited at the leading margin of the fold-thrust zone. The northeast of the Makran rotated CCW as the Indian Plate converged towards the Helmand block. Meanwhile, the north convergence of the Arabian Plate rotated the southwestern part of the MKFB CW (Fig. 9d). It is important to note that the southwestern rotation of the MKFB is slightly later than the northeast. At the same time, the final collision of the Indian Plate with the Helmand Block on the western boundary of the Indian Plate led to the expansion of the NE-SW formation and the propagation of strike-slip faults, such as the Panjgur, Hoshab, Nai Rud, and Ornach Nal faults (Figs. 5 and 8a).

The thrust and reverse faulting in the western side of the MFB is possibly accompanied by Pliocene-Pleistocene volcanic activity in the CRA region (Khan et al., 2026). In the Pliocene, the northward subduction of the Indian Plate shortened the extrusion of the MKFB, in which the northeast of the MKFB rotated CCW by ~50° (Klootwijk et al., 1981), and the southeast of the Afghan Block to the northwest of Balochistan also rotated CCW by 43° to 63° due to the Indian Plate subduction. In the southwest, the convergence of the Arabian Plate caused MKFB to rotate CW by 18° to 40°, forming a large number of small strike-slip faults and reverse thrusts (Fig. 5).

The oblique collision of the Late Cenozoic Indian Plate-Helmand block resulted in a tectonic reversal of the MKFB from sedimentation to uplifting (Treloar and Izatt, 1993). At the western edge of the Indian Plate, the MKFB, parallel to the Sulaiman Fold Belt, developed extrusion shortening (Fig. 9d). Since the Pleistocene strata covered the deformed MKFB strata, the lower Pliocene unit is folded with the rest of the sequence (Treloar and Izatt, 1993). It is worth noting that most of the MKFB shortening likely occurred during the Pliocene–Pleistocene.

6. Limitations of the study

This preliminary study is constrained by: (1) a limited number of sampling sites (seven), (2) the absence of fold tests, (3) a lack of baked contact tests, and (4) basin-wide extrapolation from localized data. Future work should include more sites, isotopic dating, and 3-D modeling.

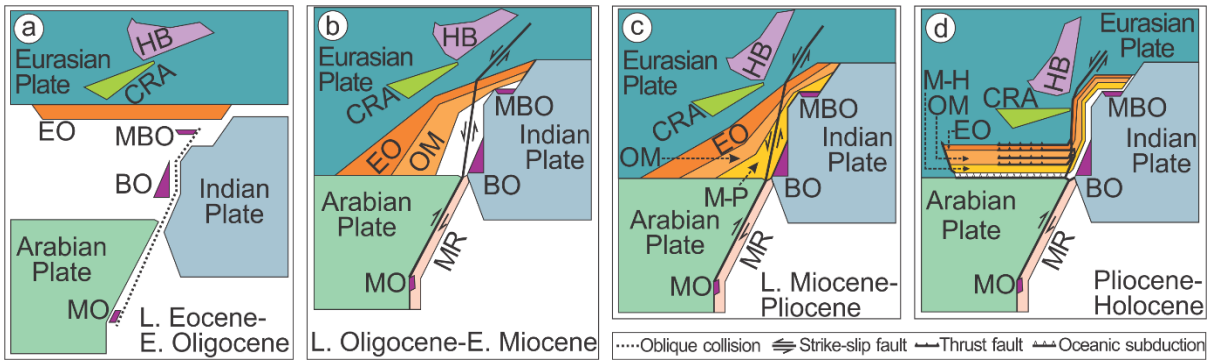

Fig. 9. The newly adapted tectonic model (a) the tectonic evolution from late Eocene to early Oligocene, (b) the tectonic evolution from late Oligocene to early Miocene, (c) the tectonic evolution from late Miocene to Pliocene, and (d) the tectonic evolution from Pliocene to Holocene. HB: Helmand Block, CRA: Chagai-Raskoh Arc, MBO: Muslimbagh Ophiolite, BO: Bela Ophiolite, MO: Masirah Ophiolite, EO: late Eocene to early Oligocene (Murgha Faqirzai Formation/Hoshab Shale), OM: late Oligocene to early Miocene (Shaigalu Formation/Panjgur Formation), and M-P: Miocene to Holocene (including Parkini, Chatti, Gwadar, and other formations).

7. Conclusion

This study concludes with the following main findings:

- The CW rotations and left-lateral motion of the east-west fault may have resulted from the subduction of the Arabian plate below MFB and the associated tectonic stress and strain distribution. The CCW rotations and left-lateral motion of the north-south fault are related to the north-westward movement of the Indian plate.
- From the late Eocene to the early Miocene, the displacement rate was low. Since the Miocene, the displacement rate has increased significantly. The continuous oblique convergence of the Indian plate has formed a series of north-south left-lateral fault systems, represented by the Chaman fault, the Ghazaband fault, and the ONF, which regulate the deformation between the Indian plate and the Eurasian plate and play the role of transform faults. At the same time, these faults spread out to the south and west, forming a series of faults that turn from north to south to east-west in MFB, such as Panjgur, Hoshab, Nai Rud, ONF, and other faults. With the left-lateral rotation of the north-south fault, the initial complete MKFB split into MFB and KFB, which also led to the displacement of ophiolites and the formation of the Y-shaped suture junction.
- During the Paleocene to the early Eocene, the MKFB was an east-west arc-trench basin, and during the late Eocene to early Oligocene, as the Indian plate moved north, the Paleo-Indus River west of the Indian plate transported debris to the MKFB arc-trench basin, and the MKFB began the sedimentation process. The earliest deposits were the TOMF, which underwent strike-slip deformation to form the Hoshab Shale. During the Late Oligocene to Miocene, the TOMP was deposited, and from the Miocene, the MFB began to strongly fold and thrust, and a new sedimentary cycle began at its leading edge, mainly from the early fold-thrust uplift zone, turning the basin into a self-maintained sedimentary basin.

Acknowledgements

We express our gratitude to Professor Jie Liu, Professor Xiaodong Tan, Dr. Linyu Han, as well as the dedicated team at our university laboratory, for their invaluable support throughout the course of our experiments. This study was funded by the National Natural Science Foundation of China (41572178, 42272250) and the Guangdong Basic and Applied Research Foundation (2023A1515011812).

Authors' Contribution

Waseem Khan proposed the main concept, did field work, collected samples, analyzed laboratory experiments, and was involved in write up. Ke Zhang supervised, funded, provided relevant literature, and reviewed and proof read of the manuscript. Ziying Li, Mahnoor Mirwani, Jiangtao Nie, Jian Guo, and Shazia Fareed did a technical review before submission and proofreading of the manuscript. Hao Liang, funded and did a technical review before submission and proofreading of the manuscript.

Data Availability Statement

Datasets used in this study are available with Dr. Waseem Khan.

Conflicts of Interest

The authors declare no conflict of interest.

Declaration of Funding

This research received no specific funding from any public, commercial, or not-for-profit agencies.

References

Bande, A., Sobel, E. R., Mikolaichuk, A., Schmidt, A., & Stockli, D. F. (2017). Exhumation history of the western Kyrgyz Tien Shan: Implications for intramontane basin formation. *Tectonics, 36*(1), 163–180. https://doi.org/10.1002/2016TC004284

Besse, J., & Courtillot, V. (1988). Paleogeographic maps of the continents bordering the Indian Ocean since the Early Jurassic. *Journal of Geophysical Research, 93*(B10), 11791. https://doi.org/10.1029/JB093iB10p11791

Bosboom, R., Dupont-Nivet, G., Huang, W., Yang, W., & Guo, Z. (2014). Oligocene clockwise rotations along the eastern Pamir: Tectonic and paleogeographic implications. *Tectonics*, *33*(2), 53–66. https://doi.org/10.1002/2013TC003388

Burtman, V. S. (2013). The geodynamics of the Pamir-Punjab syntaxis. *Geotectonics*, *47*(1), 31–51. https://doi.org/10.1134/S0016852113010020

Butler, R. F. (1992). *Paleomagnetism: Magnetic domains to geologic terranes* (Vol. 319). Blackwell Scientific Publications.

Cogné, J. P. (2003). PaleoMac: A Macintosh™ application for treating paleomagnetic data and making plate reconstructions. *Geochemistry, Geophysics, Geosystems*, *4*(1), 1007. https://doi.org/10.1029/2001GC000227

Copley, A., Avouac, J. P., & Royer, J. Y. (2010). India-Asia collision and the Cenozoic slowdown of the Indian plate: Implications for the forces driving plate motions. *Journal of Geophysical Research*, *115*(B3), B03410. https://doi.org/10.1029/2009JB006634

Cowgill, E. (2010). Cenozoic right-slip faulting along the eastern margin of the Pamir salient, northwestern China. *Geological Society of America Bulletin*, *122*(1–2), 145–161. https://doi.org/10.1130/B26520.1

Cowgill, E., Yin, A., Harrison, T. M., & Xiao-Feng, W. (2003). Reconstruction of the Altyn Tagh fault based on U-Pb geochronology: Role of back thrusts, mantle sutures, and heterogeneous crustal strength in forming the Tibetan Plateau. *Journal of Geophysical Research: Solid Earth*, *108*(B7). https://doi.org/https://doi.org/10.1029/2002JB002080

Critelli, S., De Rosa, R., & Platt, J. P. (1990). Sandstone detrital modes in the Makran accretionary wedge, southwest Pakistan: implications for tectonic setting and long-distance turbidite transportation. *Sedimentary Geology*, *68*(4), 241–260. https://doi.org/10.1016/0037-0738(90)90013-J

Delisle, G., von Rad, U., Andruleit, H., von Daniels, C., Tabrez, A., & Inam, A. (2002). Active mud volcanoes on- and offshore eastern Makran, Pakistan. *International Journal of Earth Sciences, 91*(1), 93–110. https://doi.org/10.1007/s005310100203

Dewey, J. F., & Casey, J. F. (2011). The origin of obducted large-slab ophiolite complexes. In *Arc-continent collision* (pp. 431-444). Berlin, Heidelberg: Springer

Berlin Heidelberg. https://doi.org/10.1007/978-3-540-88558-0_15

Ellouz-Zimmermann, N., Deville, E., Müller, C., Lallemant, S., Subhani, A. B., & Tabreez, A. R. (2007). Impact of sedimentation on convergent margin tectonics: Example of the Makran accretionary prism (Pakistan). In *thrust belts and foreland basins: From fold kinematics to hydrocarbon systems* (pp. 327-350). Berlin, Heidelberg: Springer Berlin Heidelberg. https://doi.org/10.1007/978-3-540-69426-7_17

Fisher, R. (1953). Dispersion on a Sphere. *Proceedings of the Royal Society A: Mathematical, Physical and Engineering Sciences*, *217*(1130), 295–305. https://doi.org/10.1098/rspa.1953.0064

Gaina, C., van Hinsbergen, D. J. J., & Spakman, W. (2015). Tectonic interactions between India and Arabia since the Jurassic reconstructed from marine geophysics, ophiolite geology, and seismic tomography. *Tectonics*, *34*(5), 875–906. https://doi.org/10.1002/2014TC003780

Gnos, E., Khan, M., Mahmood, K., Khan, A. S., Shafique, N. A., & Villa, I. M. (1998). Bela oceanic lithosphere assemblage and its relation to the Réunion hotspot. *Terra Nova*, *10*(2), 90–95. https://doi.org/10.1046/j.1365-3121.1998.00173.x

Haq, S. S. B., & Davis, D. M. (1997). Oblique convergence and the lobate mountain belts of western Pakistan. *Geology*, *25*(1), 23–26. https://doi.org/10.1130/0091-7613(1997)025<0023:OCATLM>2.3.CO;2

Hunting Survey Corporation. (1960). *Reconnaissance geology of part of West Pakistan: a Colombo Plan Cooperative Project*. Government of Canada for the Government of Pakistan.

Immenhauser, A., Schreurs, G., Gnos, E., Oterdoom, H. W., & Hartmann, B. (2000). Late Palaeozoic to Neogene geodynamic evolution of the northeastern Oman margin. *Geological Magazine*, *137*(1), 1–18. https://doi.org/10.1017/S0016756800003526

Jadoon, I. A. K., & Frisch, W. (1997). Hinterland-Vergent Tectonic Wedge Below the Riwat Thrust, Himalayan Foreland, Pakistan: Implications for Hydrocarbon Exploration. *AAPG Bulletin*, *81*(3), 1320–1336. https://doi.org/10.1306/522B4375-1727-11D7-8645000102C1865D

Kakar, D. M., Kasi, A. K., Kassi, A. M., Friis, H., Mohibullah, M., & Khan, S. (2016). Petrography and Whole-Rock Geochemistry of the Oligocene-Miocene Khojak Formation Khojak-Pishin Belt, Pakistan: Implications on Provenance and Source Area Weathering. *Journal of Himalayan Earth Science*, *49*(2), 137-157. http://ojs.uop.edu.pk/jhes/article/view/1923

Kassi, A. M., Grigsby, J. D., Khan, A. S., & Kasi, A. K. (2015). Sandstone petrology and geochemistry of the Oligocene–Early Miocene Panjgur Formation, Makran accretionary wedge, southwest Pakistan: Implications for provenance, weathering and tectonic setting. *Journal of Asian Earth Sciences*, *105*, 192–207. https://doi.org/10.1016/j.jseaes.2015.03.021

Kassi, A. M., Kasi, A. K., McManus, J., & Khan, A. S. (2013). Lithostratigraphy, petrology and sedimentary facies of the Late Cretaceous-Palaeocene Ispikan Group, southwestern Makran, Pakistan. *Journal of Himalayan Earth Sciences*, *46*(2), 49–63.

Kassi, A. M., Khan, A. S., Kelling, G., & Kasi, A. K. (2011). Facies and cyclicity within the Oligocene-Early Miocene Panjgur Formation, Khojak–Panjgur Submarine Fan Complex, south-west Makran, Pakistan. *Journal of Asian Earth Sciences*, *41*(6), 537–550. https://doi.org/10.1016/j.jseaes.2011.03.007

Khan, M., Kerr, A. C., & Mahmood, K. (2007). Formation and tectonic evolution of the Cretaceous–Jurassic Muslim Bagh ophiolitic complex, Pakistan: Implications for the composite tectonic setting of ophiolites. *Journal of Asian Earth Sciences*,

31(2), 112–127. https://doi.org/10.1016/j.jseaes.2007.04.006

Khan, W., Zhang, K., Li, Z., Liang, H., Nie, J., & Guo, J. (2026). Magnetic fabric analysis of the Makran–Khojak flysch belt (Pakistan) based on AMS data. *Carbonates Evaporites. 41*, 14. https://doi.org/10.1007/s13146-025-01216-8

Khan, W., Zhang, K., Liang, H., & Yu, P. (2023a). Geochemical Assessment of River Sediments at the Outlets of Eastern Makran, Pakistan; Implications for Source Area Weathering and Provenance. *Minerals*, *13*(3), 348. https://doi.org/10.3390/min13030348

Khan, W., Zhang, K., Liang, H., & Yu, P. (2023b). Provenance for the Makran Flysch Basin in Pakistan: implications for interaction between the Indian, Eurasian, and Arabian Plates. *Journal of Asian Earth Sciences*, 248, 105626. https://doi.org/10.1016/j.jseaes.2023.105626

Klootwijk, C. T., Nazirullah, R., DeJong, K. A., & Ahmed, H. (1981). A palaeomagnetic reconnaissance of northeastern Baluchistan, Pakistan. *Journal of Geophysical Research*, *86*(B1), 289–306. https://doi.org/10.1029/JB086iB01p00289

Koymans, M. R., Langereis, C. G., Pastor-Galán, D., & van Hinsbergen, D. J. J. (2016). Paleomagnetism.org: An online multi-platform open source environment for paleomagnetic data analysis. *Computers & Geosciences*, *93*, 127–137. https://doi.org/10.1016/j.cageo.2016.05.007

Lawrence, R. D., Yeats, R. S., Khan, S. H., Farah, A., & DeJong, K. A. (1981). Thrust and strike slip fault interaction along the Chaman transform zone, Pakistan. *Geological Society, London, Special Publications*, *9*(1), 363–370. https://doi.org/10.1144/GSL.SP.1981.009.01.33

Mahmood, K., Boudier, F., Gnos, E., Monié, P., & Nicolas, A. (1995). $^{40}Ar/^{39}Ar$ dating of the emplacement of the Muslim Bagh ophiolite, Pakistan. *Tectonophysics*, *250*(1–3), 169–181. https://doi.org/10.1016/0040-1951(95)00017-5

Molnar, P., & Stock, J. M. (2009). Slowing of India's convergence with Eurasia since 20 Ma and its implications for Tibetan mantle dynamics. *Tectonics*, *28*(3), TC3001. https://doi.org/10.1029/2008TC002271

Mouchot, N., Loncke, L., Mahieux, G., Bourget, J., Lallemant, S., Ellouz-Zimmermann, N., & Leturmy, P. (2010). Recent sedimentary processes along the Makran trench (Makran active margin, off Pakistan). *Marine Geology*, *271*(1–2), 17–31. https://doi.org/10.1016/j.margeo.2010.01.006

Reiter, K., Kukowski, N., & Ratschbacher, L. (2011). The interaction of two indenters in analogue experiments and implications for curved fold-and-thrust belts. *Earth and Planetary Science Letters*, *302*(1–2), 132–146. https://doi.org/10.1016/j.epsl.2010.12.002

Robinson, A. C., Yin, A., Manning, C. E., Harrison, T. M., Zhang, S. H., & Wang, X. F. (2004). Tectonic evolution of the northeastern Pamir: Constraints from the northern portion of the Cenozoic Kongur Shan extensional system, western China. *Geological Society of America Bulletin*, *116*(7), 953–973. https://doi.org/10.1130/B25375.1

Suo, Y., Li, S., Cao, X., Dong, H., Li, X., & Wang, X. (2022). Two-stage eastward diachronous model of India-Eurasia collision: Constraints from the intraplate tectonic records in Northeast Indian Ocean. *Gondwana Research*, *102*, 372–384. https://doi.org/10.1016/j.gr.2020.01.006

Sussman, A. J., Butler, R. F., Dinarès-Turell, J., & Vergés, J. (2004). Vertical-axis rotation of a foreland fold and implications for orogenic curvature: an example from the Southern Pyrenees, Spain. *Earth and Planetary Science Letters*, *218*(3–4), 435–449. https://doi.org/10.1016/S0012-821X(03)00644-7

Tapponnier, P., Mattauer, M., Proust, F., & Cassaigneau, C. (1981). Mesozoic

ophiolites, sutures, and arge-scale tectonic movements in Afghanistan. *Earth and Planetary Science Letters*, *52*(2), 355–371. https://doi.org/10.1016/0012-821X(81)90189-8

Tapponnier, P., Peltzer, G., & Armijo, R. (1986). On the mechanics of the collision between India and Asia. *Geological Society, London, Special Publications*, *19*(1), 113–157. https://doi.org/10.1144/GSL.SP.1986.019.01.07

Tapponnier, P., Peltzer, G., Le Dain, A. Y., Armijo, R., & Cobbold, P. (1982). Propagating extrusion tectonics in Asia: New insights from simple experiments with plasticine. *Geology*, *10*(12), 611–616. https://doi.org/10.1130/0091-7613(1982)10<611:PETIAN>2.0.CO;2

Treloar, P. J., & Izatt, C. N. (1993). Tectonics of the Himalayan collision between the Indian Plate and the Afghan Block: a synthesis. *Geological Society, London, Special Publications*, *74*(1), 69–87. https://doi.org/10.1144/GSL.SP.1993.074.01.06

Ul-Hadi, S. (2012). Multidisciplinary investigations of the Chaman strike-slip fault along the western Indo-Asian collision boundary, Pakistan. Doctoral dissertation, University of Houston. http://hdl.handle.net/10657/602

van Hinsbergen, D. J., Steinberger, B., Doubrovine, P. V., & Gassmöller, R. (2011). Acceleration and deceleration of India-Asia convergence since the Cretaceous: Roles of mantle plumes and continental collision. *Journal of Geophysical Research: Solid Earth*, *116*(B6), B06101. https://doi.org/10.1029/2010JB008051

Zhang, Z., & Sun, J. (2020). Cenozoic tectonic rotations in different parts of the NE Pamir: implications for the evolution of the arcuate orogen. *International Journal of Earth Sciences*, *109*(6), 1921–1939. https://doi.org/10.1007/s00531-020-01880-2